Annals of Biomedical Engineering, Vol. 23, pp. 697–704, 1995
Printed in the USA. All rights reserved.

0090-6964/95 $10.50 + .00

Biomechanical Topography of Human Ankle Cartilage

K. A. ATHANASIOU, G. G. NIEDERAUER, and R. C. SCHENCK, JR.

Orthopedic Biomechanics Laboratory, Department of Orthopedics, The University of Texas Health Science Center at San Antonio, San Antonio, TX

Abstract—The material properties of normal cadaveric human cartilage in the ankle mortice (tibiotalar articulation) were evaluated to determine a possible etiologic mechanism of cartilage injury of the ankle when an obvious traumatic episode is not present. Using an automated indentation apparatus and the biphasic creep indentation methodology, creep indentation experiments were performed in five sites in the distal tibia, one site in the distal fibula, and eight sites in the proximal talus of 14 human ankles (seven pairs). Results showed significant differences in the mechanical properties of specific human ankle cartilage regions. Topographically, tibial cartilage is stiffer (1.19 MPa) than talar cartilage (1.06 MPa). Cartilage in the anterior medial portion of the tibia has the largest aggregate modulus (H_A = 1.34 MPa), whereas the softest tissue was found to be in the posterior lateral (0.92 MPa) and the posterior medial (0.92 MPa) regions of the talus. The posterior lateral ridge of the talus was the thickest (1.45 mm) and the distal fibula was the thinnest (0.95 mm) articular cartilage. The largest Poisson's ratio was found in the distal fibula (0.08). The lowest and highest permeability were found in the anterior lateral regions of the astragalus (0.80×10^{-15} $m^4N^{-1}sec^{-1}$) and the posterior medial region of the tibia (1.79×10^{-15} $m^4N^{-1}sec^{-1}$), respectively. The anterior and posterior regions of the lateral and medial sites of the tibia were found to be 18–37% stiffer than the anatomically corresponding sites in the talus. The biomechanical results may explain clinically observed talar dome osteochondral lesions when no obvious traumatic event is present. Cartilage lesions in a repetitive overuse process in the ankle joint may be related to a disparity of mechanical properties between the articulating surfaces of the tibial and talar regions.

Keywords—Tibiotalar joint, Articular cartilage, Material properties, Creep indentation, KLM biphasic theory.

INTRODUCTION

The tibiotalar or ankle joint has been described as a mortice and pestle-like articulation (Fig. 1). The tibial mortice is created by the tibiofibular complex with the medial malleolus and fibula forming the sides of the mortice of the ankle. The talus is covered with over 75% hyaline cartilage and receives its blood supply through ligamentous insertions. The tibiotalar mortice has an intimate articulation producing joint stability. The posterior portion of the talus is narrower in the medial-lateral plane than that anterior-posterior. This anatomy dictates that immobilization of the ankle be performed in neutral position such that the widest portion is articulating with the tibial mortice. Both ligamentous and bony attachments provide inherent joint stability with muscular control compensating for ligamentous injuries.

Damage to the articular surfaces of the ankle joint is less common than that of the knee or hip, but is equally disabling. The human ankle is afflicted with many pathologic degenerative processes, which are mostly manifested in the talus. These pathologic changes are usually associated with transchondral fractures of the talus, osteochondritis dissecans of the talus, and osteoarthritis of tibial and talar surfaces usually secondary to trauma.

Nonidiopathic ankle osteoarthritis has been related to fracture, malalignment, or the aging process. In general, degenerative changes of articular cartilage are thought to be associated with biomechanical (1,9,12,22,28), biochemical (14,22,28), or pathological (18,22) factors. Altered joint mechanics, such as a mechanical insult or low-level repetitive insult, may lead to osteoarthritis (18) or other types of degenerative changes. In the human hip for example, degenerative changes occur most frequently in the inferior aspects of the femoral head and in the superior aspect of the acetabular dome and are thought to be due to a disparity in biomechanical properties of the articulating surfaces (4). Progressive changes consistent with osteoarthritis were observed in the operated knee and hip of guinea pigs after altering their gait and weight-bearing (2). Comparisons of articular cartilage of the human femoral head of the hip and the talus of the ankle have indicated that, as patient age increases, the incidence of osteoarthritis occurring in the hip and knee joints increases, whereas osteoarthritis rarely occurs in the ankle except as secondary to a traumatic episode (15). In the ankle, anterior osteophytes of the talus and tibia are frequent early signs of tibiotalar cartilage degeneration.

Osteochondritis dissecans of the talus has been defined as a subchondral lesion of a small bone fragment where the overlying cartilage is intact or fractured (25). Consequently, this fragment becomes separated from the surrounding bed and becomes loose within the affected joint

Address correspondence to K. A. Athanasiou, Orthopedic Biomechanics Laboratory, Department of Orthopedics, The University of Texas Health Science Center, 7703 Floyd Curl Drive, San Antonio, Texas 78284-7774, U.S.A.

(Received 8Jun94, Revised 29Nov94, Revised 13Feb95, Accepted 21Mar95)

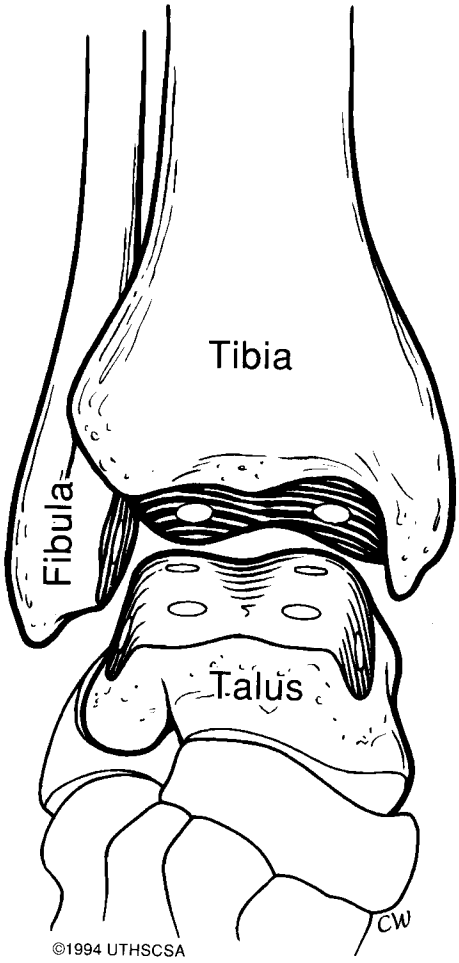

FIGURE 1. Anatomical drawing of tibiotalar joint. Test sites examined are depicted by open circles.

(25). Many theories regarding the cause of osteochondritis dissecans have been proposed including vascular, traumatic, hereditary, and constitutional factors. The posteromedial and anterolateral aspects of the talus are the most frequent sites of osteochondritis dissecans (25). Transchondral fractures have been implicated as a possible traumatic etiology of osteochondritis dissecans with well-defined mechanisms of injury.

Transchondral fractures of the talus (6) occur most frequently in the anterolateral or mid- and posteromedial portions of the talar dome (27) and secondary to trauma in the anterolateral or posteromedial area of the talus (8). Generalized mechanisms of injury have been defined and widely accepted (6). For instance, the anterolateral portion is injured with inversion and dorsiflexion, whereas the posteromedial region is injured with plantarflexion and eversion. These events should be defined as macrotraumatic events such as ankle sprain or fracture-subluxation/dislocation. Interestingly, one clinical study has shown posteromedial lesions to have no traumatic event in approximately one-half of cases (29).

Biomechanically related factors that lead to cartilage damage or degeneration have been shown to include increased stresses on the cartilage (1,12), low-contact or noncontact (loading) regions on the joint surface (5,7), or use and disuse of certain portions of the joint (10). The conclusion these studies have made is that when the normal mechanical environment of the articular cartilage surface is altered, degenerative changes are observed.

In a previous study, the cartilage biomechanics of the radiocapitellar joint were investigated, and a mechanism for osteochondritis dissecans affecting the humeral capitellum was proposed (26). It was found that significant differences exist in the mechanical properties and thickness of cartilage topographically in the capitellum and radial head, and between the two surfaces. Specifically, the compressive stiffness of the articular cartilage of the midradial head (0.62 MPa) and the midlateral capitellum (0.76 MPa) were significantly different, which may introduce mechanical mismatches leading to increased strain in the lateral capitellum (26). As a result, the increased strain may be a factor in the initiation and localization of the dissecans lesion observed in osteochondritis dissecans of the elbow during high valgus-stress activities such as throwing. Furthermore in a study of the human hip, the acetabular and femoral head cartilage show significant mismatches in mechanical properties, which correspond with sites of frequent pathological degeneration (4). For example, the superomedial aspect of the femoral head has an aggregate modulus (1.82 MPa), which is 41% higher than that of the superomedial portion of the acetabulum (1.28 MPa). These observations led us to investigate the ankle joint and determine whether similar mechanical mismatches exist there.

The goal of this study was to biomechanically evaluate the articulating surfaces of the normal ankle topographically (tibia, talus, fibula) in order to identify possible mechanisms for the observed pathologic conditions affecting the ankle. The intrinsic material properties (aggregate modulus, H_A; Poisson's ratio, ν_s; permeability, k; and shear modulus, μ_s) of articulating cartilage in the distal tibia, proximal talus, and distal fibula were obtained and compared.

Clinically, patients have been observed to have anterolateral and posteromedial osteochondritis dissecans lesions with no history of trauma and no obvious injury other than aerobic activities (16). Although not proven in this study, it may be possible that with repetitive compression activities (pounding sports, jogging), osteochondritis dissecans lesions may result due to a biomechanical cartilage mismatch. The experimental protocol was designed specifically to evaluate clinically significant pathologic areas of the human tibia and talus.

MATERIALS AND METHODS

Fourteen paired fresh-frozen human cadaveric ankles (seven left and seven right) were tested. Four subjects

were female, and three were male. The average age was 51 years (range, 18–82 years). The gender and ages of the subjects were: female (50 years), female (18 years), male (72 years), female (82 years), male (68 years), female (38 years), and male (28 years). After shipment of frozen specimens to us, they were immediately placed at −80°C until time of disarticulation and specimen preparation.

Before dissection, each ankle was thawed (normal saline containing protease inhibitors: N-ethyl malemide, 10 mM; benzamidine HCl, 5 mM; EDTA, 2 mM; and PMSF, 1 mM) at room temperature for 12 hr. The preparation and testing of specimens required two freeze-thaw cycles, which are not believed to affect the tissue's intrinsic materials properties (4,13,19). The soft tissue of the ankle was removed, and dissection of the ankle was performed using a band saw under continual irrigation (Fig. 2). With the specimens thawed, an anterior midline incision was performed to remove all soft tissues surrounding the foot and ankle joint except for ligamentous and capsular structures. Thereafter, the tibiotalar joint was incised circumferentially, and the proximal ankle mortice (tibia and fibula) were osteotomized into six specimens. Top portion of Fig. 3 shows the locations of these osteochondral specimens: anterior lateral (AL), anterior medial (MA), medial malleolus (MM), posterior medial (PM), and posterior lateral (PL). The central portion of the distal fibula (FI) was also studied. Thereafter, the talus was osteotomized into eight respective segments in a midaxial position without injuring the subtalar, tibiotalar, or talonavicular articulating surfaces. The sections of each talar dome (also known as *astragalus* [*a*]) are shown in the bottom portion of Fig. 3: anterior lateral (*a*AL), central lateral (*a*CL), posterior lateral (*a*PL), side lateral (*a*SL), anterior medial (*a*AM), central medial (*a*CM), posterior medial (*a*PM), and side medial (*a*SM). Specimens were wrapped in gauze soaked in normal saline and stored at −80°C in double sealed plastic bags until time of testing.

An automated creep indentation apparatus (3,4) was used to quantify the *in situ* creep and recovery deformation behavior of each osteochondral specimen. All articular surfaces were morphologically examined grossly using the India ink staining technique to identify normal areas for indentation tests (21). The extent of degenerative changes observed in the ankle was minimal to none, although it should be pointed out that surface fibrillation is sometimes difficult to detect using the India ink staining technique. In this specimen population, there was no India ink staining evidence of any gross damage, nor of any grossly identifiable lesions of osteoarthritis. A total of 196 osteochondral specimens were tested. The testing apparatus was able to load and unload the cartilage specimen automatically through a closed-loop control system. To test, each osteochondral specimen was thawed for half an hour in normal saline containing protease inhibitors and then attached

FIGURE 2. (a) A photograph of a typical dissected ankle. (b) A close-up photograph of the exposed joint, where the tibiotalar articulation is clearly seen.

with cyanoacrylate cement to a sample holder. A fiberoptic positioning system in line with the loading shaft emitted light on the section of the articular surface to be tested. The sample holder was then positioned with a spherical joint and lead screw assembly, until the reflected light indicated that the loading shaft was normal to the cartilage surface. This procedure was accomplished within 20 sec. A tare load of 0.03 N was then applied with a 1.5 mm diameter, flat-ended, cylindrical rigid, porous indenter tip, and the tissue was allowed to reach tare creep equi-

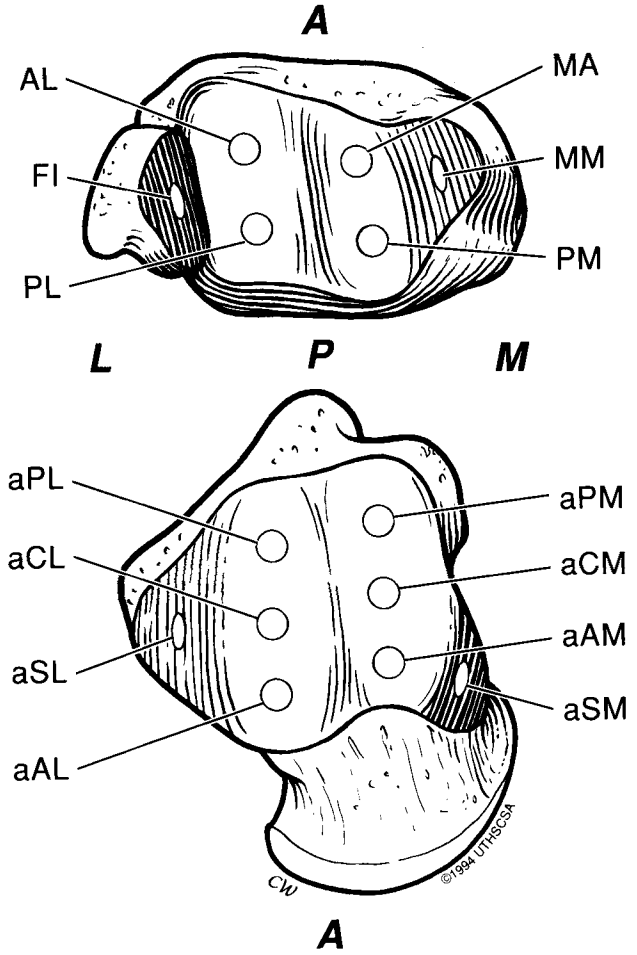

FIGURE 3. On the top, the distal tibial surface shows the dissection areas of the six specimens based on anatomical position. On the bottom, the talar dome surface shows the dissection areas of the eight specimens based on anatomical position.

librium. Equilibrium was automatically determined when the slope of the creep curve became smaller than 1×10^{-6} mm sec^{-1}. Once creep equilibrium was reached, the tissue was loaded with a step force of 0.16 N. The tissue's deformation was monitored with a linear variable differential transformer, LVDT, using a computer-based data acquisition system at a 0.25-μm deformation-resolution. Data points were collected and plotted on the screen every 2.5 μm or every 100 sec, whichever occurred first. Data acquisition and control software were written using an icon based environment (4). The frictional resistance of the system was reduced with air bearings to less than 9.81×10^{-4} N. The bearings were driven with pressurized air (552 kPa) and cleaned with a 5-μm particle filter and two 0.1-μm coalescing filters. The creep response of the specimen under the step force was monitored until equilibrium (slope $<1\times 10^{-6}$ mm sec^{-1}). At this point, the force was automatically removed, and the recovery phase began. When recovery equilibrium was achieved, data acquisition stopped and the thickness of the tissue at each test site was measured using a needle attached to a LVDT and a force transducer. Overall, the automated creep indenter yielded the creep and recovery deformational behaviors of each osteochondral specimen in response to a 0.16 N step load.

The creep indentation problem of articular cartilage, under a frictionless, porous, rigid, tip used to apply a step load, was solved using the linear KLM biphasic theory (24) by Mak and associates (17). Mow and colleagues have developed a numerical algorithm to curve-fit the indentation data using a bicubic spline function, which represents the "master solution" of the problem (23). Briefly, a numerical tabulation of the master solution was listed, and from this all other solutions can be obtained using a similarity principle. It was shown that these solutions can be acquired by simply shifting the master solutions along the log-time axis (23). The described solution scheme allows simultaneous computation of the three intrinsic properties of soft hydrated tissues: the aggregate modulus—H_A (measure of compressive stiffness); Poisson's ratio—ν_s, (apparent compressibility); and permeability—k. This methodology has been used with the creep indentation experiment to successfully obtain the intrinsic material properties of articular cartilage (3–5,23,26). In this study, the methodology was used to obtain the *in situ* intrinsic material properties and their topographical variations in the tibia, talus and fibula. The shear modulus, μ_s, was calculated from the aggregate modulus, H_A, and Poisson's ratio, ν_s, using the following equation:

$$\mu_s = \frac{H_A}{2} \cdot \frac{(1 - 2\nu_s)}{(1 - \nu_s)}$$

Donor variability and the effects of location, side (right; left), site (posterior; side; central; anterior; malleolus), structure (tibia; fibula; talus) on the material properties, thickness, creep equilibrium time, recovery equilibrium time, and percent recovery were examined using analysis of variance (ANOVA). Fisher's Least Significant Difference (FLSD) multiple comparisons test of the means was applied when the F-test in ANOVA was significant. The Student's t test was performed to look at the differences between anatomic structures, sides, and gender. The statistical significance level was set at $p < 0.05$ for all tests.

RESULTS

The mean ± standard deviation values of the intrinsic material properties (H_A, ν_s, k, μ_s) and thickness (h) of articular cartilage in the distal tibia and proximal talus are shown in Tables 1 and 2, respectively. Statistical analyses

TABLE 1. Material properties and thickness (mean ± standard deviation) of articular cartilage in the distal tibia of human ankle.

Location	H_A (MPa)	ν_s	$k \times 10^{15}$ ($m^4N^{-1}sec^{-1}$)	μ_s (MPa)	h (mm)
AL (n = 14)	1.20 ± 0.25	0.02 ± 0.04	1.55 ± 1.79	0.59 ± 0.13	1.30 ± 0.25
MA (n = 14)	1.34 ± 0.58	0.03 ± 0.06	1.41 ± 2.23	0.65 ± 0.30	1.23 ± 0.27
MM (n = 14)	0.94 ± 0.36	0.04 ± 0.08	0.93 ± 0.84	0.45 ± 0.17	0.97 ± 0.16
PM (n = 14)	1.23 ± 0.33	0.03 ± 0.07	1.79 ± 2.24	0.60 ± 0.17	1.20 ± 0.29
PL (n = 14)	1.26 ± 0.31	0.00 ± 0.01	1.56 ± 1.74	0.63 ± 0.15	1.21 ± 0.25
FI (n = 14)	1.14 ± 0.48	0.08 ± 0.08	1.32 ± 2.21	0.52 ± 0.24	0.95 ± 0.17

showed significant differences in certain biomechanical properties topographically in the tibia and talus, and between the articulating surfaces. Cartilage in the MA portion of the tibia had the largest aggregate modulus (H_A = 1.34 MPa). The softest tissue was in the *a*PL (0.92 MPa) and *a*PM (0.92 MPa) regions of the talus. Overall, tibial cartilage was slightly stiffer (p = 0.09) than talar cartilage (1.19 *versus* 1.06 MPa). The posterior aspects of the tibia combined together were stiffer than the posterior aspects of the talus (1.25 *versus* 0.92 MPa). No statistical differences were shown between the aggregate moduli of male *versus* female specimens, between left *versus* right specimens, or between medial *versus* lateral specimens.

The largest Poisson's ratio, a measure of the tissue's apparent compressibility, was in the FI (ν_s = 0.08). Statistical differences were found between the Poisson's ratio of male (0.01) *versus* female (0.04) specimens. Fibular specimens had a significantly higher Poisson's ratio (0.08) than both tibia and talar structures (0.02 and 0.02, respectively). Overall, the mean Poisson's ratio of the malleolar sites was significantly higher than the central, side, and posterior sites. Furthermore, the Poisson's ratio of the anterior sites (AL, MA, *a*AM) was significantly higher than the side sites (*a*SM, *a*SL) or posterior sites (PM, PL, *a*PL, *a*PM).

The *a*AL regions were found to be the least permeable (0.80×10^{-15} $m^4N^{-1}sec^{-1}$), whereas the PM region of the tibia was found to be most permeable (1.79×10^{-15} $m^4N^{-1}sec^{-1}$). Statistical differences were also found between the permeability of male (0.80 $m^4N^{-1}sec^{-1}$) *versus* female (1.56 $m^4N^{-1}sec^{-1}$) specimens. The highest shear modulus was in the MA region of the tibia (0.65 MPa), whereas the lowest shear moduli were in the MM regions of the tibia (0.45 MPa) and the *a*MP regions of the talar dome (0.45 MPa).

The thickest and thinnest tissues were in the *a*PL ridge of the talus (1.45 mm) and the FI (0.95 mm), respectively. A significant difference in cartilage thickness was found between male (1.40 mm) *versus* female (1.02 mm) specimens. Grouped into sites, the posterior, central and anterior sites were found to be significantly thicker than the malleolus region.

The overall recovery rate (95 ± 5.6%) was high thus indirectly verifying the India ink staining results that indeed only apparently normal surfaces were tested. For each structure (tibia, talus and fibula) and overall, the creep time was significantly larger than the recovery time (the overall mean creep time was 2394 ± 1411 sec and the mean recovery time was 1664 ± 843 sec). In this study, the creep equilibrium time under the same tare load varies from 983 to 3805 sec indicating that an *a priori* assumed fixed amount of time under the tare load, test load or recovery equilibrium, may be insufficient for articular cartilage to achieve creep equilibrium (4). Consequently, equilibrium time for tare load, test load, and recovery should be determined using slope-based criteria.

DISCUSSION

Although, osteoarthritis in the ankle is not as common as in the hip or knee (15), this joint develops degenerative changes which may be secondary to traumatic episodes or

TABLE 2. Material properties and thickness (mean ± standard deviation) of articular cartilage in the proximal talus of human ankle.

Location	H_A (MPa)	ν_s	$k \times 10^{15}$ ($m^4N^{-1}sec^{-1}$)	μ_s (MPa)	h (mm)
αAL (n = 14)	1.02 ± 0.36	0.06 ± 0.08	0.80 ± 0.65	0.47 ± 0.17	1.01 ± 0.31
αCL (n = 14)	1.21 ± 0.39	0.02 ± 0.05	0.96 ± 0.51	0.59 ± 0.19	1.17 ± 0.27
αSL (n = 14)	1.08 ± 0.42	0.00 ± 0.01	0.98 ± 0.39	0.54 ± 0.21	1.14 ± 0.23
αPL (n = 14)	0.92 ± 0.33	0.00 ± 0.00	1.05 ± 0.67	0.46 ± 0.16	1.45 ± 0.42
αPM (n = 14)	0.92 ± 0.36	0.02 ± 0.05	1.18 ± 1.39	0.45 ± 0.18	1.31 ± 0.26
αCM (n = 14)	1.25 ± 0.51	0.00 ± 0.01	1.17 ± 0.38	0.63 ± 0.26	1.31 ± 0.33
αSM (n = 14)	1.05 ± 0.29	0.02 ± 0.05	1.64 ± 2.37	0.52 ± 0.15	1.18 ± 0.24
αAM (n = 14)	1.01 ± 0.47	0.04 ± 0.05	0.94 ± 0.62	0.48 ± 0.24	1.17 ± 0.34

osteochondritis dissecans in both the talar and tibial surfaces. The intrinsic material properties between the articulating surfaces of normal cadaveric human ankle cartilage were determined at various locations to examine whether the site-specificity of cartilage degeneration of the ankle could be related to a disparity in the material properties. The results indicate that significant topographical variations exist in cartilage material properties and thickness, especially in the tibia and the talus. These biomechanical results may suggest that clinically observed injuries or pathologies occurring in specific portions of the joint may correspond with mismatches in cartilage mechanical properties. Dissimilar strain fields are produced by a disparity in the mechanical properties between two articulating surfaces. As a result, one side of the articular surface is exposed to a more strenuous mechanical environment. Consequently, degenerative changes on one side of the joint surface may be accelerated due to the larger strain fields.

Significant differences were found in the material properties among the three structures. Tibial cartilage was stiffer than talar cartilage. Fibular cartilage had a larger Poisson's ratio than tibial and talar cartilage, which indicates a propensity for more fluid transport through the solid matrix of the tibial and talar cartilage (5).

In anatomical position, the significantly softer aPM articulates with the stiffer PM. Although speculative, it is possible that pathological changes in the posteromedial aspects of the talus may be initiated by a disparity in cartilage mechanical properties. Our results show no differences in stiffness between the anterolateral talar and tibial articulation, or the medial talar dome and the midportion of the tibia. These findings agree with clinical observations that localized osteochondritis dissecans of the medial dome of the talus is probably secondary to avascular necrosis and not due to a mechanical mismatch of the articulating cartilages. Transchondral fractures in the anterolateral portion are due to inversion and dorsiflexion of the ankle which impacts the lateral aspect of the talus against the articular surface of the fibula. Similarly, ankle trauma in plantarflexion and eversion can result in a transchondral fracture in the posteromedial talus as well. Frequently, however, no history of trauma is present with lesions in this position. From our results, an additional mechanism of mechanical mismatch may be responsible for some of the "osteochondritic" lesions present in the posteromedial aspect of the talus in those patients with no history of trauma as described by Canale (29). It is possible that a "grinding mechanism" (20), may be generated between two articulating surfaces, as a result of a mismatch in the compressive modulus, which may contribute to abrasion (4). Such a mismatch may affect joint lubrication and accentuate the detrimental effects of transarticular impact loads on cartilage degeneration.

Although only six male and eight female ankles were tested in this study, cartilage of all female specimens grouped together is 94% more permeable, has 63% higher apparent compressibility, and is 27% thinner than male cartilage. However, no difference in the aggregate modulus means for the two genders was found. Previous reports on the mechanical properties of the hip found no statistically significant differences in the mechanical properties of articular cartilage between male and female specimens (4). More studies to examine the effect of gender on mechanical properties need to be undertaken to elucidate any differences.

As seen in Table 3 and Fig. 4, the material properties and thickness of human ankle articular cartilage differ from those found in the elbow (26), hip (4), and knee (5). Specifically, the aggregate modulus of ankle cartilage was 8% lower than that in the hip and 39% and 85% higher than that in the elbow or knee, respectively. Hip cartilage was twice as stiff as the knee. Similar results were obtained for the shear modulus. These differences in aggregate and shear moduli of the various joints are indicative of the different mechanical environments and functional requirements of these joints. Human articular cartilage in the knee was twice as thick as the ankle, elbow, or hip. No statistical significant differences were found in the Poisson's ratio of these four joints. The Poisson's ratio of human articular cartilage obtained in the ankle as well as in the hip (4), elbow (26), and knee (5) were significantly lower than the Poisson's ratio values of animal cartilage in the hip (monkey, cow, and dog) (3) and knee (cow, dog, monkey, and rabbit) (5). This indicates that the apparent compressibility of human articular cartilage is significantly higher than cartilage from the animals tested. In earlier reports, Poisson's ratio values ranging from 0.3 to

TABLE 3. Comparison of material properties and thickness (mean ± standard deviation) of human ankle, elbow, hip, and knee cartilage.

Joint	ν_s	$k \times 10^{15}$ ($m^4N^{-1}sec^{-1}$)	μ_s (MPa)	h (mm)
Ankle (n = 196)	0.03 ± 0.05	1.23 ± 1.47	0.54 ± 0.21	1.18 ± 0.29
Elbow (n = 132)	0.07 ± 0.08	1.29 ± 1.04	0.37 ± 0.13	1.13 ± 0.31
Hip (n = 140)	0.05 ± 0.06	0.90 ± 0.54	0.57 ± 0.30	1.34 ± 0.38
Knee (n = 14)	0.06 ± 0.07	1.45 ± 0.61	0.28 ± 0.07	2.63 ± 1.04

For aggregate modulus values, refer to Fig. 4.

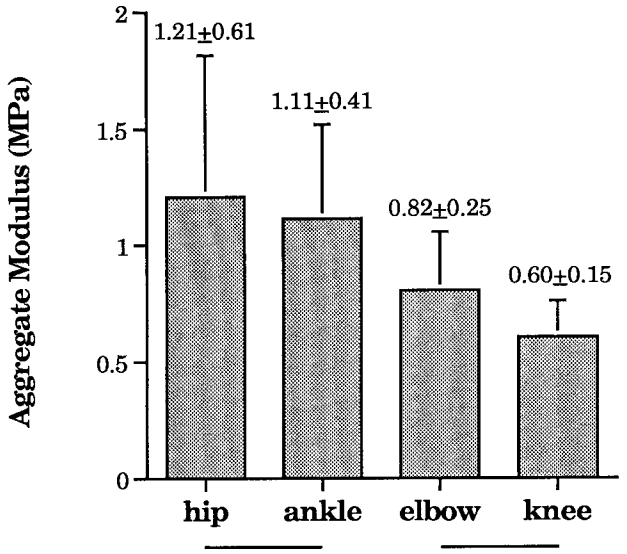

FIGURE 4. Comparison of cartilage aggregate modulus (compressive stiffness) of hip (4), ankle, elbow (26), and knee (5). Underline below graph connect mean values which have no statistically significant differences.

0.4 were given for human cartilage (11,13). In our studies, we found it to be closer to zero. For humans, the least permeable cartilage was in the hip, and the most permeable cartilage was in the knee ($p < 0.05$). The results of this study show that relatively smaller differences in cartilage material properties are seen topographically in the ankle than in the knee or hip (3–5). This is in agreement with Kempson's study (15), where it is postulated that osteoarthritic changes are significantly rarer in the ankle than in the hip or knee joints. These differences may be explained by the fact that the mismatches observed in the ankle are less pronounced than in the hip and knee.

In conclusion, the results reported in this study demonstrate significant topographical differences in the mechanical properties of human ankle cartilage. Although the objective of this study was not to quantitatively correlate biomechanical disparities to pathological cases, we can nevertheless hypothesize as to the mechanical causes underlying clinically observed problems, especially osteochondritis dissecans affecting the posteromedial portion of the talus (29). This new information adds to our knowledge of ankle biomechanics, and may provide new insights in human ankle pathophysiology as related to mechanical factors.

REFERENCES

1. Afoke, N., P. Byers, and W. Hutton. Contact pressures in the human hip joint. *J. Bone Joint Surg.* 69-B:536–541, 1987.
2. Arsever, C., and G. Bole. Experimental osteoarthritis induced by selective myectomy and tendotomy. *Arthr. Rheum.* 29:251–261, 1986.
3. Athanasiou, K., A. Agrawal, A. Muffoletto, F. Dzida, G. Constantinides, and M. Clem. Biomechanical properties of hip cartilage in experimental animal models. *Clin. Ortho. Rel. Res.* 316:254–266, 1995.
4. Athanasiou, K. A., A. Agarwal, and F. J. Dzida. Comparative study of the intrinsic mechanical properties of the human acetabular and femoral head cartilage. *J. Ortho. Res.* 12:340–349, 1994.
5. Athanasiou, K. A., M. P. Rosenwasser, J. A. Buckwalter, T. I. Malinin, and V. C. Mow. Interspecies comparisons of *in situ* intrinsic mechanical properties of knee joint cartilage. *J. Ortho. Res.* 9:330–340, 1991.
6. Berndt, A. L., and M. Harty. Transchondral fractures (osteochondritis dissecans) of the talus. *J. Bone Joint Surg.* 41-A:988–1020, 1959.
7. Bullough, P., J. Goodfellow, and J. O'Connor. The relationship between degenerative changes and load-bearing in the human hip. *J. Bone Joint Surg.* 55-B:746–758, 1973.
8. Davidson, A. M., H. D. Steele, D. A. MacKenzie, and J. A. Penny. A review of twenty-one cases of transchondral fracture of the talus. *J. Trauma* 7:378–415, 1967.
9. Day, W., S. Swanson, and M. Freeman. Contact pressures in the loaded human cadaver hip. *J. Bone Joint Surg.* 57-B:302–313, 1975.
10. Gunn, D. R. Squatting and osteoarthritis of the hip. *J. Bone Joint Surg. (Proc. Br. Ortho. Assoc.)* 46:156, 1964.
11. Hayes, W., and L. Mockros. Viscoelastic properties of human articular cartilage. *J. Appl. Physiol. 31:562–568, 1971.*
12. Hodge, W., K. Carlson, S. Fijan, S. Burgess, P. Riley, W. Harris, and R. Mann. Contact pressures from an instrumented hip endoprosthesis. *J. Bone Joint Surg.* 71-A:1378–1386, 1989.
13. Hori, R. Y., and L. F. Mockros. Indentation tests of human articular cartilage. *J. Biomech.* 9:259–268, 1976.
14. Kempson, G. E. The mechanical properties of articular cartilage. In: *Textbook of Rheumatology*, edited by L. Sokoloff. Philadelphia: W. B. Saunders, 1980, pp. 177–238.
15. Kempson, G. E. Age-related changes in the tensile properties of human articular cartilage: a comparative study between the femoral head of the hip joint and the talus of the ankle joint. *Biochim. Biophys. Acta.* 1075:223–230, 1991.
16. King, R. E., and D. F. Powell. Injury to the Talus. In: *Disorders of the Foot and Ankle: Medical and Surgical Management*, edited by M. H. Jahss. Philadelphia: W. B. Saunders, 1991, pp. 2293–2325.
17. Mak, A. F., W. M. Lai, and V. C. Mow. Biphasic indentation of articular cartilage—I. Theoretical analysis. *Biomechanics* 20:703–714, 1987.
18. Mankin, H. J., V. C. Mow, J. A. Buckwalter, J. P. Iannotti, and A. Ratcliffe. Form and function of articular cartilage. In: *Orthopaedic Basic Science*, edited by S. S. Simon. Columbus, OH: American Academy of Orthopaedic Surgeons, 1994, pp. 1–44.
19. Maroudas, A. The permeability of articular cartilage. *J. Bone Joint Surg.* 50-B:166–177, 1968.
20. Meachim, G. Articular cartilage lesions in osteo-arthritis of the femoral head. *J. Pathol.* 107:199–210, 1972.
21. Meachim, G., and I. H. Emery. Cartilage fibrillation in shoulder and hip joints in Liverpool necropsies. *J. Anat.* 116:161–179, 1973.
22. Moskowitz, R., and V. Goldberg. Osteoarthritis. In: *Primer*

on the Rheumatic Diseases, edited by H. R. Schumacher, Jr. Chicago: AMA, 1988, pp. 171–176.
23. Mow, V. C., M. C. Gibbs, W. M. Lai, W. B. Zhu, and K. A. Athanasiou. Biphasic indentation of articular cartilage—II. A numerical algorithm and an experimental study. *Biomechanics* 22:853–861, 1989.
24. Mow, V. C., S. C. Kuei, W. M. Lai, and C. G. Armstrong. Biphasic creep and stress relaxation of articular cartilage in compression: theory and experiments. *J. Biomech. Eng.* 102:73–84, 1980.
25. O'Farrell, T. A., and B. G. Costello. Osteochondritis dissecans of the talus. *J. Bone Joint Surg.* 64-B:494–497, 1982.
26. Schenck, R. C., K. A. Athanasiou, G. Constantinides, and E. Gomez. A biomechanical analysis of articular cartilage of the human elbow and a potential relationship to osteochondritis dissecans. *Clin. Ortho. Rel. Res.* 299:305–312, 1994.
27. Shelton, M. L., and W. J. Pedowitz. Injuries to the talar dome, subtalar joint, and midfoot. In: *Disorders of the Foot and Ankle: Medical and Surgical Management*, edited by M. H. Jahss. Philadelphia: W. B. Saunders, 1991, pp. 2274–2292.
28. Solomon, L. Patterns of osteoarthritis of the hip. *J. Bone Joint Surg.* (*Br.*) 58:176–183, 1976.
29. Canale, S. T., R. H. Belding: Osteochondrial lesions of the Talus. *J Bone Joint Surg* 62A:97–102, 1980.